Resonant two-photon ionization spectroscopy of coinage metal trimers: Cu_2Ag, Cu_2Au, and CuAgAu

Gregory A. Bishea, Caleb A. Arrington, Jane M. Behm,[a] and Michael D. Morse
Department of Chemistry, University of Utah, Salt Lake City, Utah 84112

(Received 5 June 1991; accepted 3 September 1991)

The jet-cooled coinage metal triatomic molecules Cu_2Ag, Cu_2Au, and CuAgAu have been investigated using resonant two-photon ionization spectroscopy. One band system, labeled as the $\tilde{A}$–$\tilde{X}$ system, has been observed for each species, with origin bands at 13 188, 17 217, and 17 470 cm^{-1}, respectively. Vibrational progressions have been assigned and vibrational constants have been extracted using a linear least-squares fitting procedure. For Cu_2Ag, 47 vibrational bands have been assigned within the $\tilde{A}$–$\tilde{X}$ system. The upper states of these bands derive from combinations of two symmetric (a_1) and one antisymmetric (b_2) mode in the C_{2v} point group. For the $\tilde{A}$–$\tilde{X}$ system of Cu_2Au, only seven vibrational bands have been observed, all occurring within a 500 cm^{-1} range. Lifetime measurements for the observed vibrational levels support the possibility that predissociation may be occurring in the $\tilde{A}$ excited state of Cu_2Au and this may be limiting the number of vibrational levels observed within this state. Finally, in the case of CuAgAu, 92 vibrational bands have been assigned, corresponding to excitations of three totally symmetric (a') vibrational modes in the C_s point group. For this molecule, a complete set of vibrational frequencies (ω_i) and anharmonicities (x_{ij}) have been obtained for the excited $\tilde{A}$ state. In addition, the observation of weak hot bands in the spectrum permits the three vibrational modes of the $\tilde{X}$ ground state to be characterized by $\nu_1 = 222.83 \pm 0.29$, $\nu_2 = 153.27 \pm 0.22$, and $\nu_3 = 103.90 \pm 0.28$ cm^{-1} for $^{63}Cu^{107}Ag^{197}Au$ (1σ error limits).

I. INTRODUCTION

A major unsettled question in physical chemistry concerns the electronic structure of metallic systems as a function of size. Atoms, on the one hand, are generally well understood and can be calculated accurately using the methods of *ab initio* quantum chemistry. Infinite metallic solids, on the other hand, are rather well understood through the methods of solid state physics, although perhaps not quite to the same degree as are isolated atoms. The intermediate range in size from the isolated atom to the bulk infinite solid, however, is by comparison characterized very poorly. As a result, major efforts in many research groups are currently directed toward understanding the development of bulk metallic properties as one moves from the isolated metal atom to the bulk infinite solid. The fundamental questions concern how the geometrical structure of a small cluster evolves into the stable crystal structures of the bulk, how the electronic energy levels of a small cluster evolve into the band structure of the solid, and how the characteristic reactions of the surface of the bulk solid phase are modified as one moves to smaller clusters.

Among the various experimental methods used to probe the properties of metal clusters are photoelectron spectroscopy of mass-selected metal cluster anions,[1–10] photofragmentation spectroscopy of mass-selected metal cluster cations,[11–16] measurements of ionization potentials and electron affinities as functions of cluster size,[17–20] measurements of the reactivity and reaction equilibria for metal clusters interacting with various ligating molecules,[21–24] electron-spin resonance (ESR),[25–29] and resonance Raman spectroscopy[30,31] of matrix-isolated metal clusters, resonant two-photon ionization spectroscopy of metal dimers and trimers,[32–36] and resonant two-photon ionization photoelectron spectroscopy of metal dimers.[37,38] Some of these techniques are extremely well suited for the study of metallic properties as functions of cluster size, but in most cases, the more detailed spectroscopic probes have been limited to diatomic, or possibly triatomic systems.

Only a few triatomic metals have been investigated spectroscopically with any sort of success in the gas phase. To our knowledge, the only examples where vibrational structure has been resolved and analyzed are the alkali clusters Li_3,[39] Na_3,[40–49] and Li_xNa_{3-x},[50,51] the coinage metal (pseudoalkali) clusters Cu_3 (Refs. 52–55) and Ag_3,[56] the *p*-block metal Al_3,[57] and the transition metal cluster Ni_3.[58] The attention received by the alkali and coinage metal trimers stems in part from the relatively simple electronic structure of these species, which possess only one valence electron per atom in their ground electronic states. In addition to this relatively simple electronic structure, the low boiling points of the alkali metals permit relatively high pressures of alkali atoms to be generated in an alkali oven and this has contributed substantially to the relative ease of spectroscopic studies of the alkali trimers. Even within the alkali and coinage metals, however, many triatomic species still remain spectroscopic mysteries.

The homonuclear alkali and coinage metal trimers are all expected to possess ground electronic states of $\tilde{X}\,^2E'$ in the D_{3h} point group, deriving from the molecular orbital configuration $a_1'^2e'^1$. Here both the a_1' and e' orbitals consist

[a] Kodak Fellow.

primarily of linear combinations of the valence *ns* atomic orbitals on the three metal centers. Of course, the $\tilde{X}\,^2E'$ state is orbitally degenerate and is therefore subject to a Jahn–Teller distortion which lowers the symmetry from D_{3h} to C_{2v}. This distortion breaks the degeneracy of the $\tilde{X}\,^2E'$ state into $^2A_1$ and $^2B_2$ states in C_{2v} symmetry. In some of the alkali and coinage metal homonuclear trimers, the energy stabilization obtained by this distortion is thought to be minor, leading to molecules which undergo pseudorotation readily. In addition, many of the excited electronic states of these species are also orbitally degenerate $^2E'$ or $^2E''$ states at the D_{3h} geometry, and these are subject to Jahn–Teller distortion as well. Because they have the fewest number of atoms which can still generate a Jahn–Teller effect, the homonuclear alkali and coinage metal trimers offer one of the simplest examples of this effect.

In a previous series of papers, we have reported the results of spectroscopic investigations of the coinage metal diatomics Cu_2,[59] CuAg,[60] CuAu,[61,62] AgAu, and Au_2,[62,63] and we have reported spectroscopic results on Cu_3 as well.[52,55] In this paper, we extend these studies to the mixed triatomic systems Cu_2Ag, Cu_2Au, and CuAgAu. Although it is impossible for these heteronuclear species to achieve a D_{3h} geometry, the analogy between the chemical bonding of these molecules and that of the homonuclear trimers suggests that conical intersections should be present in these species as well. Thus, e.g., the ground states of Cu_2Ag and Cu_2Au should possess C_{2v} symmetry and should either belong to the $^2A_1$ or $^2B_2$ symmetry species. Just as these states become degenerate at the equilateral (D_{3h}) geometry in homonuclear molecules such as Li_3, Na_3, and Cu_3, these two states should also become degenerate at some geometry for molecules such as Cu_2Ag and Cu_2Au. The possibility of obtaining evidence of such conical intersections provided part of the motivation for the present investigation.

In Sec. II, we present a brief overview of the experimental methods employed in this investigation. Section III provides the results, which are discussed further in Sec. IV. A summary of our most important findings is then given in Sec. V.

II. EXPERIMENTAL

The experimental methods employed in this investigation combine four separate techniques: laser vaporization of metal alloys; supersonic expansion in an inert carrier gas; resonant two-photon ionization spectroscopy; and time-of-flight mass spectrometry. The metal cluster beam was formed by focusing the second harmonic of a *Q*-switched Nd:YAG laser (532 nm, 15–20 mJ/mm^2) onto a metal target surface in the throat of a pulsed supersonic expansion of helium. The ejected atoms were then entrained in a pulsed flow of helium (120 psi), which carried them through a channel 2 mm in diameter and 2 cm in length. Experiments were then performed with various extension channels, which were added to lengthen this channel prior to the final supersonic expansion into vacuum, in the hope of improving the production of the triatomic molecules Cu_2Ag, Cu_2Au, and CuAgAu. Ultimately, an extension channel 6 mm in length, tapering from a 5 mm initial inside diameter down to a 1.5 mm exit orifice was chosen. The small exit orifice also promoted excellent supersonic cooling, so that low rotational temperatures and narrow vibronic bands were obtained.

Two metal targets were prepared by melting the weighed metals in an electric arc. One consisted of an equimolar alloy of copper and silver, while the second consisted of an equimolar alloy of copper, silver, and gold. After allowing the molten metal mixtures to solidify and cool, the light yellow alloys were pressed flat and polished to give disk-shaped samples approximately 2 mm in thickness and 2.5 cm in diameter. These were then suitable for pulsed laser vaporization using a rotating disk mount similar to that described by O'Brien *et al.*[64]

Following expansion into vacuum, the supersonically cooled molecular beam passed through a 5 mm skimmer and entered the ionization region of a reflectron time-of-flight mass spectrometer. There the metal clusters were probed using a Nd:YAG pumped tunable dye laser (5–15 mJ/cm^2) for excitation and a fixed frequency excimer laser (either KrF at 5.00 eV, or ArF at 6.42 eV) for photoionization of the excited molecules. The ions produced in this resonant two-photon ionization process were then mass analyzed in a time-of-flight mass spectrometer, allowing spectra to be gathered independently for each isotopic modification of the molecule. The ion signal was amplified, digitized, and signal averaged, with the entire experimental cycle repeating at a rate of 10 Hz. Optical spectra of the species of interest were obtained by monitoring the ion intensity of a particular mass peak as a function of scanning dye laser wavelength. Rotationally resolved studies were not possible using the present Nd:YAG-pumped pulsed dye laser system, but will be possible in the near future in this laboratory using a commercial cw ring dye laser system.

For the CuAgAu molecule, one band was examined under high resolution (0.03 cm^{-1}) in order to establish an accurate calibration of the dye laser. This was accomplished by narrowing the output of the dye laser by the insertion of an air-spaced intracavity etalon, which was then pressure scanned with SF_6 while an absorption spectrum of gaseous I_2 was recorded simultaneously. The I_2 atlas of Gerstenkorn and Luc[65] was then used to provide an absolute frequency calibration for this band. As a result, all of the band positions reported for CuAgAu are probably correct to within 1 cm^{-1}. Corresponding corrections were applied to the frequencies of the Cu_2Ag and Cu_2Au band positions, but these may be in error by a slightly greater amount. For Cu_2Au, this error is not likely to exceed 5 cm^{-1}, but the spectrum of Cu_2Ag falls in a very different spectral range and errors for this species may be as much as 10 cm^{-1}.

Measurements of excited state lifetimes were performed by recording the ion signal as a function of the delay time between the firing of the excitation laser and the photoionization laser. The resulting decay curves were fitted to an exponential decay function by a nonlinear least-squares algorithm,[66] allowing the upper state lifetimes to be extracted.

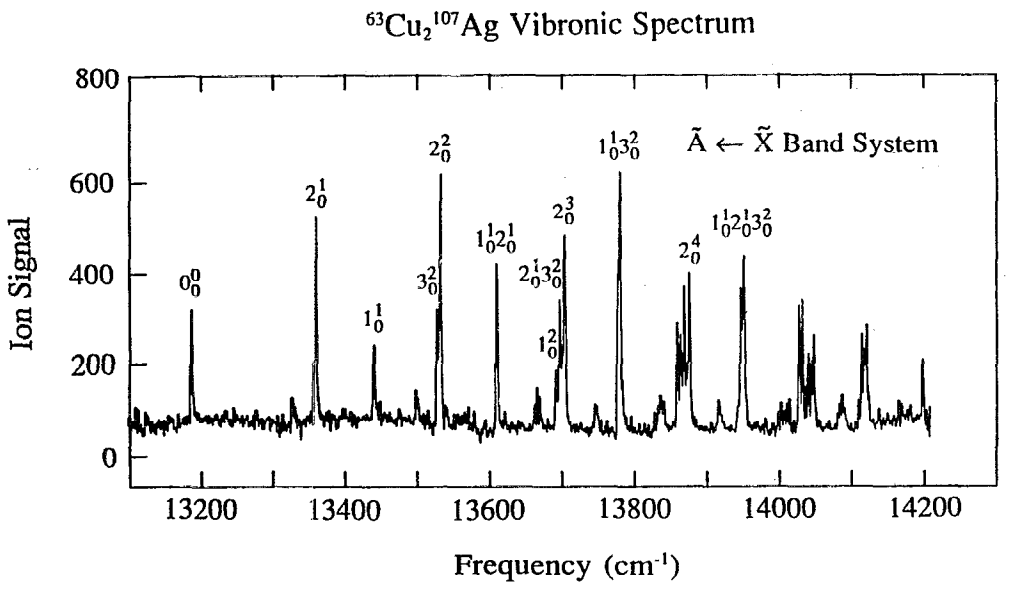

FIG. 1. Low resolution scan of the $\tilde{A} \leftarrow \tilde{X}$ band system of Cu_2Ag, recorded using LDS 750 and 751 dye laser radiation in combination with KrF excimer radiation for photoionization. A near coincidence of the vibrational frequencies of mode 2 (of a_1 symmetry in C_{2v}) and mode 3 (of b_2 symmetry in C_{2v}) causes higher vibrational levels of the $\tilde{A}$ state to appear to be split into multiplets. This is further exacerbated because two quanta of mode 1 (of a_1 symmetry in C_{2v}) nearly match the energy of three quanta of either mode 2 or 3.

TABLE I. Vibronic bands of the $\tilde{A}$–$\tilde{X}$ system of $^{63}Cu_2{}^{107}Ag$.[a]

Band	Frequency (cm^{-1})[b]	Isotope shift (cm^{-1})[c]			
		$^{63}Cu_2{}^{109}Ag$[d]	$^{63}Cu^{65}Cu^{107}Ag$[d]	$^{63}Cu^{65}Cu^{109}Ag$	$^{65}Cu_2{}^{109}Ag$
0_0^0	13 188.34(14)	−0.58(−67)	−0.58(−145)	−0.85(−59)	−0.85(−60)
2_0^1	13 360.89(−13)[e]	−1.11(−35)	−1.11(−36)	−2.23(−29)	−2.23(−49)
1_0^1	13 441.91(133)	−1.68(59)	−1.68(125)	−3.35(50)	−3.35(90)
3_0^2	13 531.31(173)	−2.83(150)	−2.83(191)	−6.26(70)	−6.26(56)
2_0^2	13 533.20(−29)[e]	−1.57(−2)	−1.57(70)	−3.57(−5)	−3.57(16)
$1_0^1 2_0^1$	13 612.00(187)	−1.90(152)	−1.90(268)	−4.18(128)	−4.18(152)
1_0^2	13 693.80(−190)	−0.38(11)	−3.53(−199)	−4.58(8)	−4.58(−8)
$2_0^1 3_0^2$	13 699.33(−134)	−1.37(−40)	−1.37(1)	−4.52(36)	−4.52(−23)
2_0^3	13 705.22(−37)	−2.00(27)	−2.00(168)	−4.80(19)	−4.80(142)
$1_0^1 2_0^2$	13 780.72(141)	···	···	···	···
$1_0^1 3_0^2$	13 782.48(−72)	−2.94(−61)	−2.94(−2)	−6.09(−27)	−7.84(−123)
$1_0^2 2_0^1$	13 861.66(−31)	−4.04(−186)	−4.04(−59)	−8.95(−248)	−8.95(−280)
3_0^4	13 865.82(−168)	−2.38(−201)	−5.35(−378)	−7.42(−196)	···
$2_0^2 3_0^2$	13 871.16(−23)	−4.16(−254)	−4.16(−221)	−8.61(−184)	−8.61(−227)
2_0^4	13 877.70(38)	−2.97(68)	−8.61(−293)	−6.24(86)	···
$1_0^1 2_0^3$	13 948.08(−6)	−1.48(74)	−5.35(−112)	−4.75(35)	−6.83(−4)
$1_0^1 2_0^1 3_0^2$	13 952.54(153)	−3.86(−9)	−3.86(20)	−6.53(165)	−6.53(201)
$1_0^2 2_0^2$	14 029.20(132)	−2.15(161)	−2.15(304)	−7.06(105)	−7.06(118)
$2_0^1 3_0^4$	14 034.11(−272)	···	···	···	···
$1_0^2 3_0^2$	14 038.41(−113)	−1.23(142)	−1.23(115)	−7.98(38)	−7.98(111)
$2_0^3 3_0^2$	14 042.40(66)	−1.23(64)	−1.23(86)	−8.29(−4)	−8.29(28)
2_0^5	14 049.46(78)	−3.99(53)	−3.99(313)	−7.68(96)	···
$1_0^1 2_0^4$	14 115.15(−144)	−2.76(−179)	−6.14(−283)	−4.91(−71)	−7.98(−46)
$1_0^1 2_0^2 3_0^2$	14 119.14(70)	−1.23(74)	−1.23(69)	···	···
$1_0^1 3_0^4$	14 122.83(50)	···	···	−7.98(−13)	−10.13(−94)
$2_0^1 3_1^1$	13 327.69(−263)	−0.31(−94)	−0.31(−119)	···	···
3_1^1	13 499.34(133)	−1.68(238)	−1.68(273)	−2.82(148)	−2.82(98)
$2_0^1 3_1^1$	13 501.73(−18)	−2.08(0)	−2.08(7)	−2.65(−62)	−2.65(−111)
$1_0^2 3_1^1$	13 666.45(−64)	−3.84(−98)	−3.84(−105)	···	···
$2_0^1 3_1^3$	13 668.88(65)	−2.55(−18)	−2.55(−24)	···	···
$2_0^3 3_1^1$	13 671.53(−161)	−0.64(9)	−2.07(−98)	···	···
$1_0^1 2_0^2 3_1^1$	13 748.41(5)	−2.13(−4)	−2.13(29)	−3.53(−116)	−3.53(−94)
$1_0^1 3_1^3$	13 750.52(−172)	−2.13(−105)	−2.13(−114)	−3.53(−152)	−3.53(−83)
$1_0^2 2_0^1 3_1^1$	13 830.78(−172)	−1.48(−31)	−1.48(−56)	−1.87(97)	−1.87(59)
3_1^5	13 836.42(224)	−2.38(33)	−2.38(129)	−5.05(47)	−5.05(11)

TABLE I. (*Continued.*)

Band	Frequency (cm^{-1})[b]	Isotope shift (cm^{-1})[c]			
		$^{62}Cu_2{}^{109}Ag$[d]	$^{63}Cu^{65}Cu^{107}Ag$[d]	$^{63}Cu^{65}Cu^{109}Ag$	$^{65}Cu_2{}^{109}Ag$
$2_0^2 3_1^3$	13 839.39(131)	−0.30(157)	−0.30(105)	−2.78(233)	−2.78(128)
$2_0^4 3_1^1$	13 843.84(−15)	−2.97(−86)	−2.97(−28)	−5.94(−196)	−5.94(−8)
$1_0^1 2_0^3 3_1^1$	13 917.20(89)	⋯	⋯	⋯	⋯
$1_0^1 2_0^1 3_1^3$	13 921.06(188)	⋯	⋯	⋯	⋯
$1_0^2 2_0^2 3_1^1$	13 999.12(158)	⋯	⋯	⋯	⋯
$2_0^1 3_1^5$	14 003.11(46)	⋯	⋯	⋯	⋯
$2_0^3 3_1^3$	14 008.02(46)	⋯	⋯	⋯	⋯
$1_0^2 3_1^5$	14 012.01(281)	⋯	⋯	⋯	⋯
$2_0^5 3_1^1$	14 015.69(120)	⋯	⋯	⋯	⋯
$1_0^1 2_0^4 3_1^1$	14 081.08(−281)	⋯	⋯	⋯	⋯
$1_0^1 2_0^2 3_1^3$	14 084.46(−129)	⋯	⋯	⋯	⋯
$1_0^1 3_1^5$	14 087.52(−210)	⋯	⋯	⋯	⋯

[a] Vibronic bands were fit to the formula

$$\nu = T_0 + \sum_i [\omega_i' v_i' + x_{ii}'(v_i'^2 + v_i')] + \sum_{i<j} x_{ij}'[v_i' v_j' + (v_i' + v_j')/2] - \nu_3'' v_3''$$

for $v_3'' = 0,1$. The resulting values of T_0, ω_1', ω_2', ω_3', x_{11}', x_{22}', x_{33}', x_{12}', x_{13}', x_{23}', and ν_3'' are given in Table II, along with their 1σ error limits.

[b] Following each observed frequency, the residual $\nu_{obs} - \nu_{calc}$ is given in units of 0.01 cm^{-1} in parentheses.

[c] Isotope shifts are given as ν (isotope modification) $- \nu(^{63}Cu_2{}^{107}Ag)$. Following each observed isotope shift, the residual $\nu_{obs} - \nu_{calc}$ is given for the fit of that isotopic modification to the formula given in footnote a. The resulting values of the vibrational constants are given in Table II, along with their 1σ error limits.

[d] Assignments for the $^{63}Cu_2{}^{109}Ag$ and $^{63}Cu^{65}Cu^{107}Ag$ species are complicated by the fact that both species fall in the same mass peak, contributing 49.0% and 51.0%, respectively, to the intensity of this feature. The reported assignments for these species should be viewed with caution. A similar problem exists for $^{63}Cu^{65}Cu^{109}Ag$ and $^{65}Cu_2{}^{107}Ag$, but the latter species only contributes 19.4% to the intensity of the mass peak, so the reported assignment is much more definite for $^{63}Cu^{65}Cu^{109}Ag$.

[e] Lifetimes of the 010 and 020 levels of the $\tilde{A}$ state were measured by exciting the 2_0^1 and 2_0^2 bands using the time-delayed resonant two-photon ionization method. The resulting values, along with their 1σ error limits, are

$\tau(010) = 34.9 \pm 12.3$ μs, $\tau(020) = 27.2 \pm 12.6$ μs.

III. RESULTS

A. The $\tilde{A} \leftarrow \tilde{X}$ system of Cu_2Ag

Figure 1 displays the low resolution (≈ 0.5 cm^{-1}) resonant two-photon ionization spectrum of $^{63}Cu_2{}^{107}Ag$ in the energy region from 13 150 to 14 300 cm^{-1}, recorded using LDS 750 and 751 dye laser radiation in combination with KrF excimer radiation (248 nm, 5.00 eV) for photoionization. Although we have scanned from the near infrared to the near ultraviolet, this is the only band system found for Cu_2Ag. Accordingly, it is labeled as the $\tilde{A} \leftarrow \tilde{X}$ system. Vibronic band positions for the $^{63}Cu_2{}^{107}Ag$ (mass 233) isotopic modification are listed in Table I, along with isotope shifts for the mass 235 (51.0% $^{63}Cu^{65}Cu^{107}Ag$ and 49.0% $^{63}Cu_2{}^{109}Ag$), mass 237 (80.6% $^{63}Cu^{65}Cu^{109}Ag$ and 19.4% $^{65}Cu_2{}^{107}Ag$), and mass 239 ($^{65}Cu_2{}^{109}Ag$) features. Excited state lifetimes are also given for the two excited state vibrational levels where this measurement was performed. The $\tilde{A}$ state shows a very long fluorescence lifetime ($\tau \approx 30$ μs), which corresponds to an absorption oscillator strength of $f \approx 0.0003$ assuming that the decay is entirely due to fluorescence to the ground electronic state. In addition, the observation of the origin band at 13 188 cm^{-1} using a KrF excimer laser for photoionization places the ionization potential of Cu_2Ag in the range $5.00 < \text{I.P.}(Cu_2Ag) < 6.64$ eV. This system was not observed using ArF excimer radiation for photoionization, further restricting the range of ionization potential to $5.00 < \text{I.P.}(Cu_2Ag) < 6.42$ eV.

The spectrum shown in Fig. 1 for the isotopically pure species $^{63}Cu_2{}^{107}Ag$ is somewhat simpler than that obtained for the mass 235 and 237 species, which are mixtures of two isotopomers. The spectrum is quite clean at the low frequency end, where the origin band is evident, followed by a strong feature labeled as the 2_0^1 band and a weaker feature labeled as the 1_0^1 band. In this labeling scheme, the large number refers to the vibrational mode under consideration, the subscript gives the number of vibrational quanta of excitation in this mode in the lower state and the superscript gives the number of vibrational quanta excited in the upper state. At higher frequencies, however, the spectrum becomes progressively more complicated, with the band labeled as 2_0^2 appearing to be doubled, the 2_0^3 band seemingly tripled, and the 2_0^4 band apparently split into four features. Such a pattern might be expected in a homonuclear trimer, where the doubly degenerate e' bending mode may be excited with n quanta to give a single A_1' level for $n = 0$, a doubly degenerate E' level for $n = 1$, an A_1' level and a doubly degenerate E' level for $n = 2$, an A_1', an A_2', and a doubly degenerate E' level for $n = 3$, etc. This would lead to n distinct vibrational levels when the bending mode is excited with n quanta (for $n > 0$),

just as found in Fig. 1. Of course, it would be surprising to observe all of these levels, since three different vibrational symmetries are represented among these levels (A_1', A_2', and E') and selection rules would in most cases prohibit the observation of all of them. Any explanation based on such effects would seem to be out of the question for Cu_2Ag, however, since this heteronuclear molecule cannot possibly have a doubly degenerate bending mode, since it belongs to the nondegenerate, C_{2v} point group.

In C_{2v}, the Cu_2Ag molecule will have two vibrational modes of a_1 symmetry and one mode of b_2 symmetry. In an electronically allowed transition, excitations from the ground vibrational level of the $\tilde{X}$ state will only be possible if they terminate on vibrational levels of A_1 symmetry in the $\tilde{A}$ state. Thus, if we designate the two a_1 modes as modes 1 and 2, and the b_2 mode as mode 3, the only vibrational transitions which should be observed which originate from the zero-point level of the ground state are the $1_0^i 2_0^j 3_0^{2k}$ bands. Furthermore, if we use the homonuclear trimers as a model, one would expect a relatively high frequency breathing mode (of a_1 symmetry) and two nearly degenerate bending modes (of a_1 and b_2 symmetries). Labeling the breathing mode as mode 1, the a_1 bending mode (mode 2) and the b_2 bending mode (mode 3) should be nearly degenerate in frequency. One would then expect the 3_0^2 and 2_0^2 bands to be close in frequency. Accordingly, the weaker feature near the intense 2_0^2 band is assigned as the 3_0^2 band. A similar near degeneracy would be expected for the 2_0^3 and $2_0^1 3_0^2$ bands, the 2_0^4, $2_0^2 3_0^2$, and 3_0^4 bands, etc. This assignment would explain some aspects of the clumps of features, since the 2_0^2 band would appear to be doubled (with the 3_0^2 band located nearby), the 2_0^3 band would also seem doubled (with the $2_0^1 3_0^2$ band nearby), and the 2_0^4 band would be apparently tripled (with both the $2_0^2 3_0^2$ and 3_0^4 bands nearby). Although this is a good beginning for an assignment, it is not sufficient because these bands appear doubled, tripled, and quadrupled instead of doubled, doubled, and tripled, respectively.

At this point, we may note that a double excitation of the totally symmetric breathing mode (mode 1) will have an energy of $2\nu_1 \approx 502$ cm^{-1}, which is a close match to the energy of three quanta of either mode 2 or mode 3 ($3\nu_2 \approx 526$ cm^{-1}). Thus, the 2_0^3 band appears tripled because of a near degeneracy with the $2_0^1 3_0^2$ and 1_0^2 bands. Likewise, the 2_0^4 band appears quadrupled because of a near degeneracy with the $2_0^2 3_0^2$, 3_0^4, and $1_0^2 2_0^1$ bands. In the range of 14 025–14 050, an even more complex structure appears to consist of five bands, resulting from the near degeneracy of the 2_0^5, $2_0^3 3_0^2$, $2_0^1 3_0^4$, $1_0^2 2_0^2$, and $1_0^2 3_0^2$ bands. Since the upper states of these features are nearly of the same energy and have the same total vibrational symmetry, they are very likely mixed by anharmonic interactions, allowing intensity to be shared between them. Such anharmonic mixing effects are common in polyatomic molecules where vibrational levels of the same symmetry have similar energies, as was first discovered by Fermi in his investigation of the mixing of the 10^00 and 02^00 vibrational levels of CO_2.[67]

Extending the logic of the assignment presented above, it is possible to identify all of the predicted upper state vibrational levels of A_1 symmetry within 1000 cm^{-1} of the 0_0^0 band except for the 1_0^3 and the $1_0^3 2_0^1$ bands. These are predicted using the constants of the least-squares fit to lie within the clumps of bands near 13 950 and 14 120 cm^{-1}, respectively. The fitted vibrational constants are given in Table II; measured band positions and residuals are given in Table I. The weaker features in Fig. 1, which have not been labeled for clarity, are assigned as hot bands arising from excited vibrational levels of the $\tilde{X}$ ground state. These are thought to arise from a ground state molecule with one quantum of excitation in its antisymmetric bending mode ν_3, which is of b_2 symmetry. These transitions terminate on the same set of

TABLE II. Fitted vibrational constants for Cu_2Ag.[a]

State	Constant	$^{63}Cu_2{}^{107}Ag$	$^{63}Cu_2{}^{109}Ag$[b]	$^{63}Cu^{65}Cu^{107}Ag$[b]	$^{63}Cu^{65}Cu^{109}Ag$	$^{65}Cu_2{}^{109}Ag$
$\tilde{A}$	T_0	13 188.19(119)	13 188.41(111)	13 189.20(168)	13 188.07(120)	13 188.08(123)
	ω_1'	250.98(251)	249.69(267)	246.73(403)	249.53(285)	248.27(290)
	ω_2'	175.27(118)	173.38(134)	172.21(203)	172.45(146)	173.19(154)
	ω_3'	172.13(106)	168.91(135)	167.65(205)	167.87(139)	168.07(148)
	x_{11}'	1.37(64)	1.22(68)	1.75(102)	0.54(72)	1.03(74)
	x_{22}'	−0.18(14)	−0.10(17)	−0.08(26)	−0.08(18)	−0.38(21)
	x_{33}'	−0.44(13)	−0.01(18)	0.04(17)	−0.04(18)	−0.06(19)
	x_{12}'	−3.28(37)	−2.77(42)	−2.49(64)	−2.41(47)	−2.43(51)
	x_{13}'	0.61(32)	0.97(46)	1.60(69)	1.16(45)	0.90(48)
	x_{23}'	−0.87(21)	−0.16(28)	0.23(42)	−0.39(31)	−0.26(34)
$\tilde{X}$	ν_3''	200.96(56)	200.95(55)	200.44(83)	197.36(67)	197.00(71)

[a]All constants are reported in wave numbers (cm^{-1}), followed by the 1σ error limits in parentheses, given in units of 0.01 cm^{-1}. These constants were obtained by a least-squares fit of the data of Table I to the expression

$$\nu = T_0 + \sum_i [\omega_i' v_i' + x_{ii}'(v_i'^2 + v_i')] + \sum_{i<j} x_{ij}' [v_i' v_j' + (v_i' + v_j')/2] - \nu_3'' v_3''$$

for $v_3'' = 0,1$.

[b]As mentioned in footnote d of Table I, data for $^{63}Cu_2{}^{109}Ag$ and $^{63}Cu^{65}Cu^{107}Ag$ were obtained from the same mass peak and there is an associated ambiguity as to what features correspond to which species. As a result, the fitted constants should be viewed with caution.

excited state levels as do the cold bands, except with one additional quantum of excitation in the b_2 mode (mode 3). Accordingly, a weak set of features which mimic the strong features are found in the spectrum, displaced some 29 cm^{-1} to the red because of a decrease in the frequency of mode 3 by this amount upon electronic excitation of the molecule. These hot bands are reported in Table I, and have been included in a least-squares fit of the data to give a ground state vibrational frequency of 200.96 ± 0.56 cm^{-1} for the ν_3'' vibration.

Although we have been successful in accounting for all of the features in this complicated spectrum, it should be emphasized that it is not always clear which features in the clumps of bands belong to which normal mode assignments. The assignment given is very likely not unique. Indeed, each of the vibrational levels of the $\tilde{A}$ upper state lying within a given clump is probably a mix of several normal mode descriptions, due to anharmonic couplings which may strongly mix nearly degenerate levels of the same symmetry species. If this is true, the entire basis for the description of the energy levels in terms of good quantum numbers (v_1, v_2, and v_3), fundamental frequencies (ω_i), and anharmonicities (x_{ij}) is approximate at best. Thus our constants, particularly the anharmonicities (x_{ij}), should be viewed as empirical parameters which reproduce the spectrum, but do not necessarily imply the validity of the normal mode description. Within each clump of vibrational levels, a complicated mixing of the normal mode basis wave functions must almost certainly be occurring.

B. The $\tilde{A} \leftarrow \tilde{X}$ system of Cu_2Au

The entire range of visible and near infrared dyes was scanned in the search for spectra of Cu_2Au, but again only one band system was found. This is labeled as the $\tilde{A} \leftarrow \tilde{X}$ system and is displayed in Fig. 2. The apparent origin band is located at 5862 Å, which is close to the region where Ruamps reports banded spectra assigned to a polyatomic Cu_nAu molecule in a high temperature King furnace investigation.[68] This spectrum was obtained using rhodamine 590 and 610 dye laser radiation in conjunction with KrF radiation (248 nm, 5.00 eV) to provide the second, ionizing photon. Accordingly, the ionization potential of Cu_2Au may be placed above the KrF energy of 5.00 eV and below the sum of this energy and the energy of the origin band, which is 7.13 eV. Unlike the spectra of Cu_2Ag described above and CuAgAu given below, only seven bands are observed, with the entire spectrum falling within a 500 cm^{-1} region. The observed band frequencies are given in Table III along with measured excited state lifetimes, which for the 000 and 010 vibrational levels average to give $\tau = 799 \pm 90$ ns. Assuming that these levels decay entirely by fluorescence to the ground electronic state, this corresponds to an absorption oscillator strength of $f \approx 0.006$.

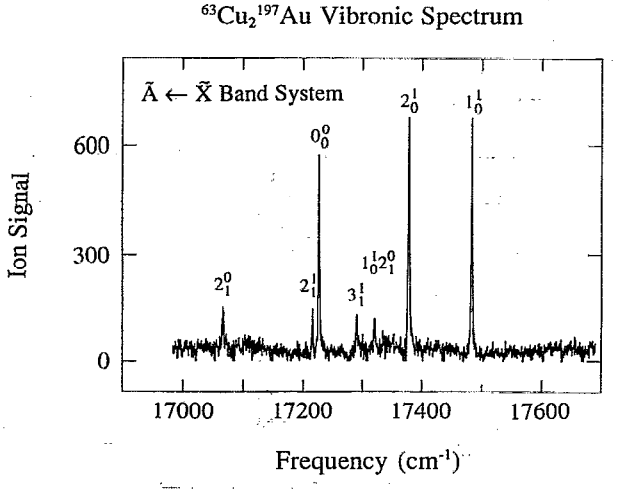

FIG. 2. Low resolution scan of the $\tilde{A} \leftarrow \tilde{X}$ band system of Cu_2Au, recorded using rhodamine 590 and 610 dye laser radiation in combination with KrF excimer radiation for photoionization. Three bands show up prominently and must originate from molecules in the zero-point level of the ground electronic state. In addition, four hot bands associated with vibrationally excited molecules in the jet-cooled molecular beam are also present. Three of these mimic the intense transitions and must originate from a common vibrational level of a_1 symmetry. See the text for details.

Three of the observed bands are intense and arise clearly from the zero-point level of the $\tilde{X}$ ground state of Cu_2Au, while the four remaining bands are much weaker and originate from vibrationally excited levels of the $\tilde{X}$ ground state. The origin band is assigned clearly at 17 217.51 cm^{-1}, but the two remaining cold bands fail to form a vibrational progression and must be assigned to excitations of two different vibrational modes of the $\tilde{A}$ state. In analogy to the results for Cu_2Ag, these are thought to correspond to excitations of the two totally symmetric modes with one quantum of excitation and are labeled as the 2_0^1 and 1_0^1 bands, in order of increasing transition frequency. The higher frequency totally symmetric mode of the excited $\tilde{A}$ state again probably corresponds to a breathing motion of the molecule and is similar in frequency to that found for Cu_2Ag (253 cm^{-1} for Cu_2Au vs 251 cm^{-1} for Cu_2Ag). The other totally symmetric mode is probably best described as a bending motion and is somewhat lower in frequency for Cu_2Au than for Cu_2Ag (149 cm^{-1} for $^{63}Cu_2{}^{197}Au$ vs 175 cm^{-1} for $^{63}Cu_2{}^{107}Ag$).

The remaining bands are all very weak and must originate from vibrationally excited Cu_2Au molecules in the ground $\tilde{X}$ state. Three of these bands mimic the three intense bands, but are shifted 159.73 cm^{-1} to the red. Accordingly, a totally symmetric vibrational level of the ground $\tilde{X}$ state of Cu_2Au must lie 159.73 cm^{-1} above the zero-point level. Presumably this value corresponds to the lowest frequency vibration of a_1 symmetry, which is probably best described as a bending mode (although some stretching character is undoubtedly present in this normal coordinate).

The remaining hot band lies at 17 280.1 cm^{-1} and must originate from a different vibrational level of the ground state. If this band originated from a totally symmetric (A_1) vibrational level of the ground state, transitions to *all* of the totally symmetric levels of the upper state would be expected and the three cold bands should be again mimicked at reduced intensity. A careful search of the baseline shows no evidence for this and an alternative explanation must be sought. Apart from the totally symmetric A_1 vibrational levels, the only other symmetry species available for a vibrational level of a C_{2v} molecule is B_2. The lowest energy vibra-

TABLE III. Vibronic bands of the $\tilde{A}$–$\tilde{X}$ system of $^{63}Cu_2{}^{197}Au$.[a]

Band	Frequency (cm^{-1})	Isotope shift (cm^{-1})[b] $^{63}Cu^{65}Cu^{197}Au$	Isotope shift (cm^{-1})[b] $^{65}Cu_2{}^{197}Au$	Lifetime[c] (ns)
2_1^0	17 057.35	+ 1.13	+ 1.32	
2_1^1	17 206.31	− 0.36	− 0.30	
0_0^0	17 217.51	− 0.12	− 0.18	744 ± 134
3_1^1	17 280.10	− 0.59	− 0.90	
$1_0^1 2_1^0$	17 311.03	− 0.95	− 0.83	
2_0^1	17 365.75	− 1.01	− 1.76	844 ± 121
1_0^1	17 470.62	− 1.68	− 3.36	331 ± 342

[a] The observed levels may be analyzed through the formula

$$\nu = T_0 + \sum_i \nu_i' v_i' - \sum_i \nu_i'' v_i'', \quad \text{for } v_i', v_i'' = 0,1.$$

The resulting constants are given in Table IV.

[b] Isotope shifts are defined as ν (isotopic modification) $- \nu(^{63}Cu_2{}^{197}Au)$.

[c] Lifetimes were measured by the time-delayed resonant two-photon ionization method. The quoted errors represent the 1σ error limit obtained from a nonlinear least-squares fit of the exponential decay curves.

tional level of this type corresponds to a single excitation of the antisymmetric b_2 vibration, which in the $\tilde{A}$ state of Cu_2Ag has a frequency of approximately 172 cm^{-1}. Assuming a similar frequency in the ground state of Cu_2Au, this is low enough that it could still be populated in a jet-cooled molecular beam. Moreover, if the weak band at 17 280.1 cm^{-1} originated from the lowest level of B_2 vibrational symmetry and the transition were still induced by the same component of the electronic transition dipole moment as the other bands, then it would have to terminate on a vibrational level of B_2 symmetry in the upper state as well. With this in mind, it seems likely that this last weak band is the 3_1^1 band, which is offset from the origin band by 62.59 cm^{-1} because the b_2 mode increases in frequency by 62.59 cm^{-1} upon electronic excitation in the $\tilde{A} \leftarrow \tilde{X}$ system of Cu_2Au. The vibrational constants of all of the isotopic forms of Cu_2Au obtained from this analysis are given in Table IV.

Finally, we must ask why the 0_0^0, 2_0^1, and 1_0^1 bands show up with no hint of diminishing intensity in this molecule, but no higher frequency bands can be found. Even including the hot bands which have been observed, only four vibrational levels of the upper $\tilde{A}$ electronic state have been located. These are the 000, 100, 010, and 001 levels, as labeled by the number of vibrational quanta excited in modes 1, 2, and 3, respectively. A possible answer to this dilemma is provided in Table III, which lists the excited state lifetimes for the observed bands. The 000 and 010 vibrational states of the $\tilde{A}$ state show lifetimes of 744 ± 134 and 844 ± 121 ns, respectively, but this is decreased in the higher energy 100 level to 331 ± 342 ns. It is quite possible that higher vibrational levels of the $\tilde{A}$ state may be predissociated and this predissociation is beginning to shorten the lifetime of the 100 vibrational level. If the predissociation rate were to increase very strongly with further vibrational excitation in the molecule, this could certainly explain the limited number of excited vibrational levels observed. Moreover, it would seem that excitation of the antisymmetric b_2 mode (mode 3) makes the predissociation process occur more rapidly, since only the lowest energy B_2 level of the $\tilde{A}$ state has been observed. The onset of predissociation in the 100 vibrational level of the $\tilde{A}$ state then places the dissociation limit of Cu_2Au at $D_0^0(\text{CuAu–Cu}) < 2.17$ eV.

TABLE IV. Fitted vibrational constants for Cu_2Au.[a]

State	Constant	$^{63}Cu_2{}^{197}Au$	$^{63}Cu^{65}Cu^{197}Au$	$^{65}Cu_2{}^{197}Au$
$\tilde{A}$	T_0	17 217.51	17 217.39	17 217.33
	ν_1'	253.40(29)	251.58(3)	250.73(80)
	ν_2'	148.60(36)	148.54(119)	147.00(34)
$\tilde{X}$	ν_2''	159.73(38)	159.61(135)	157.90(80)
	$\nu_3'(\tilde{A}) - \nu_3''(\tilde{X})$	62.59	62.12	61.87

[a] All constants are reported in wave numbers (cm^{-1}) followed by an error estimate in parentheses, given in units of 0.01 cm^{-1}. These constants were obtained by an analysis of the data of Table III using the formula

$$\nu = T_0 + \sum_i \nu_i' v_i' - \sum_i \nu_i'' v_i'', \quad \text{for } v_i', v_i'' = 0,1.$$

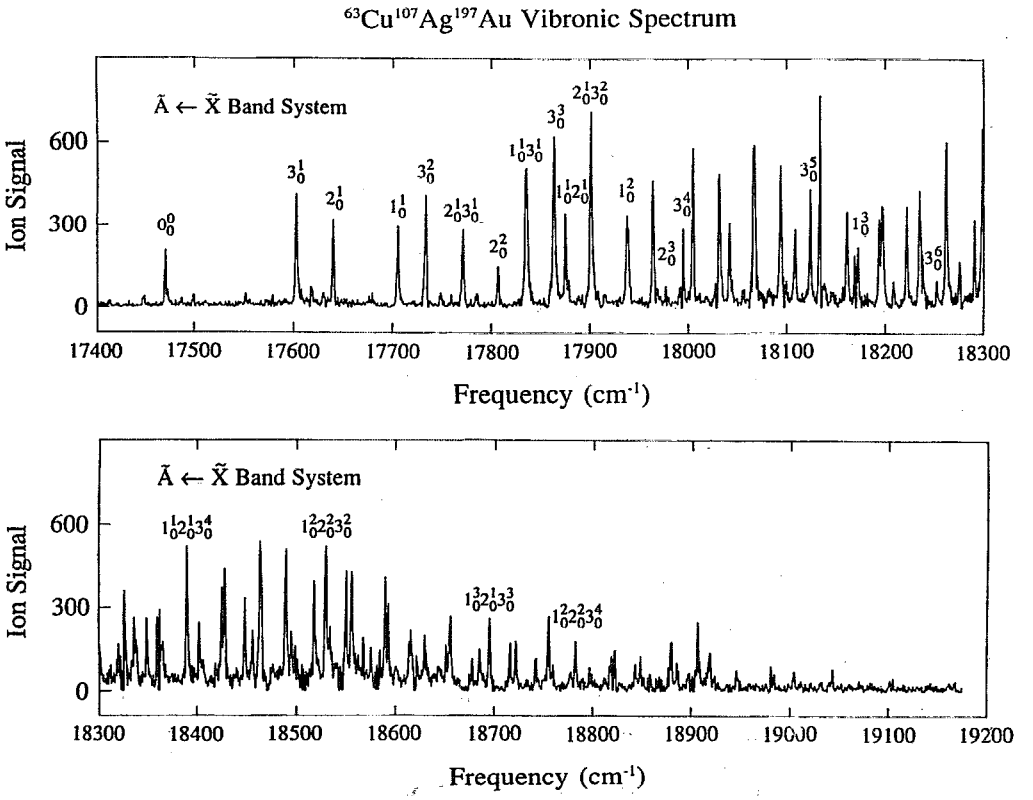

FIG. 3. Low resolution scan of the $\tilde{A} \leftarrow \tilde{X}\,^2A'$ band system of CuAgAu, recorded using rhodamine 590, fluorescein 548, coumarin 540*A*, and coumarin 500 dye laser radiation in combination with KrF excimer laser radiation for photoionization. In this molecule, which belongs to the C_s point group, all three normal modes belong to the *a'* irreducible representation, and therefore all vibrational levels are also of *A'* symmetry. As a result, all vibrational levels of the excited $\tilde{A}$ state may be accessed in the transition, resulting in the increasing complexity of the observed spectrum as it is scanned to the blue, where the density of vibrational levels in the $\tilde{A}$ state increases substantially.

C. The $\tilde{A} \leftarrow \tilde{X}$ system of CuAgAu

In contrast to the other triatomics investigated in the present work, CuAgAu belongs to the C_s, rather than the C_{2v} point group. As a result, all three of its normal modes of vibration belong to the totally symmetric representation *a'* and all three are potentially active in an electronic transition. The results of this vibrational activity are shown in Fig. 3, which presents the low resolution spectrum of $^{63}Cu^{107}Ag^{197}Au$ from 17 400 to 19 200 cm $^{-1}$. This was recorded using rhodamine 590, fluorescein 548, coumarin 540A, and coumarin 500 laser dyes in combination with KrF excimer laser radiation (248 nm, 5.00 eV) for photoionization. Since this is the only spectrum of CuAgAu observed in our scans, we assign it as the $\tilde{A} \leftarrow \tilde{X}$ system. The observed vibronic bands along with measured excited state lifetimes are given in Table V. Assuming that the upper state decays solely by fluorescence to the ground state, the measured lifetimes of 585 ± 170 and 693 ± 91 ns correspond to an absorption oscillator strength of $f \approx 0.008$. As in the cases of Cu_2Ag and Cu_2Au, the observation of the $\tilde{A} \leftarrow \tilde{X}$ band system with KrF radiation as the second, photoionizing photon and the inability to observe this system using ArF photoionizing radiation may be used to place restrictions on the ionization potential of the molecule, giving $5.00 < \text{I.P.}(\text{CuAgAu}) < 6.42$ eV.

At the red end of the spectrum, an isolated band is found, and as one moves toward the blue, the spectrum becomes more and more congested. Despite this complexity, however, the spectrum is fairly straightforward to assign once it is recognized that all three normal modes are active. As a result there are no selection rules making some vibrational levels of the upper $\tilde{A}$ state unobservable. The first peak to the blue of the origin band lies about 131 cm $^{-1}$ above it in energy. Other peaks lie 261, 391, 522, 651, and 780 cm $^{-1}$ above the origin, giving intervals between peaks of 130, 130, 131, 129, and 129 cm $^{-1}$. Although the last two of these transitions fall in a congested region where other explanations for their occurrence could certainly be found, it seems clear that a vibrational progression in one of the normal modes has been found. Since this is apparently the lowest frequency mode of the upper $\tilde{A}$ state, it is designated as ν_3, and these bands are labeled as the 3_0^1, 3_0^2, 3_0^3, 3_0^4, 3_0^5, and 3_0^6 bands. The origin band is of course labeled as 0_0^0.

Between the 3_0^1 and 3_0^2 bands, two other intense features are located. These must represent the fundamentals of the remaining two vibrational modes. Accordingly, the bands are labeled as the 2_0^1 and 1_0^1 bands, lying about 169 and 235 cm $^{-1}$ above the origin band, respectively. Progressions are again found involving mode 2, with the 2_0^2 and 2_0^3 bands lying 337 and 505 cm $^{-1}$ above the origin band, respectively, giving identical vibrational intervals of 168 cm $^{-1}$. Mode 1 also forms progressions with the 1_0^2 and 1_0^3 bands lying 468 and 698 cm $^{-1}$ above the origin band, respectively, giving vibrational intervals of 233 and 230 cm $^{-1}$.

Even with progressions in each of the three normal modes, however, it remains impossible to explain all of the features in the spectrum. Nevertheless, all of the strong features in the spectrum may be understood if combinations of

TABLE V. Vibronic bands of the $\tilde{A}$–$\tilde{X}^2A'$ system of $^{63}Cu^{107}Ag^{197}Au$.[a]

Band	Frequency (cm^{-1})[b]	Isotope shift (cm^{-1})[c]		
		$^{63}Cu^{109}Ag^{197}Au$[d]	$^{63}Cu^{107}Ag^{197}Au$[d]	$^{65}Cu^{109}Ag^{197}Au$
0_0^0	17 470.53(−31)	−0.04(−5)	−0.04(−93)	−0.04(38)
3_0^1 [e]	17 601.40(−3)	−0.40(43)	−0.40(−5)	−1.34(51)
2_0^1	17 639.11(−37)	−0.34(24)	−0.34(23)	−1.25(57)
1_0^1	17 705.16(16)	−0.75(51)	−0.75(34)	−2.82(−56)
3_0^2	17 731.80(0)	−0.71(53)	−0.71(71)	−2.13(94)
$2_0^1 3_0^1$	17 770.09(18)	−1.67(−8)	−1.67(21)	−3.74(−26)
2_0^2	17 807.17(−46)	−1.64(−38)	−1.64(−17)	−3.23(−5)
$1_0^1 3_0^1$	17 834.23(−16)	−1.58(−36)	−1.58(63)	−4.14(−69)
3_0^3	17 861.49(−42)	−1.10(−7)	−2.39(−27)	−3.94(−8)
$1_0^1 2_0^1$	17 872.74(−46)	−1.37(0)	−1.37(52)	−3.75(−59)
$2_0^1 3_0^2$	17 899.47(−63)	−1.64(−58)	−1.64(29)	−3.68(13)
$2_0^2 3_0^1$	17 938.32(44)	−3.05(−85)	−3.05(20)	−5.60(−46)
1_0^2	17 938.32(16)	−3.05(−54)	−3.05(−11)	−2.98(120)
$1_0^1 3_0^2$	17 962.84(−71)	−0.78(1)	−4.33(−113)	−5.27(−82)
2_0^3	17 975.65(38)	−2.62(35)	−2.62(15)	−4.68(77)
3_0^4	17 992.50(70)	−2.44(−24)	−5.12(−68)	−6.19(5)
$1_0^1 2_0^1 3_0^1$	18 002.40(−3)	−1.88(10)	−4.03(−45)	−5.64(−57)
$2_0^1 3_0^3$	18 029.67(−38)	−1.02(41)	−3.43(−32)	−5.04(20)
$1_0^1 2_0^2$	18 040.91(1)	−2.07(61)	−3.41(−16)	−5.82(−68)
$1_0^2 3_0^1$	18 066.58(22)	−2.27(1)	−5.76(−50)	−6.56(−44)
$2_0^2 3_0^2$	18 067.38(−52)	⋯	⋯	−4.42(86)
$1_0^1 3_0^3$	18 092.52(5)	−1.41(8)	−5.43(14)	−6.77(2)
$1_0^2 2_0^1$	18 106.72(80)	−3.81(−17)	−4.88(32)	−6.76(−35)
3_0^5	18 121.09(−35)	−1.22(−21)	−4.80(−12)	−6.28(19)
$1_0^1 2_0^1 3_0^2$	18 131.13(−28)	−1.22(52)	−5.04(−38)	−6.72(−40)
$2_0^1 3_0^4$ [e]	18 160.16(40)[e]	−2.08(6)	−4.46(43)	−6.69(52)
1_0^3	18 168.84(−150)	−2.40(−76)	−4.07(36)	−6.33(−132)
$1_0^1 2_0^2 3_0^1$	18 168.84(−111)	−1.21(42)	⋯	−4.14(132)
$1_0^2 3_0^2$	18 194.34(3)	⋯	⋯	−7.43(41)
$2_0^2 3_0^3$	18 197.87(18)	⋯	⋯	−6.57(54)
$1_0^1 2_0^3$	18 208.45(35)	⋯	⋯	⋯
$1_0^1 3_0^4$	18 221.20(5)	−1.27(−1)	−6.52(74)	−8.25(16)
$2_0^3 3_0^2$	18 234.77(−45)	⋯	⋯	−8.38(−168)
$1_0^2 2_0^1 3_0^1$	18 234.77(82)	⋯	⋯	−8.38(−11)
3_0^6	18 250.50(−35)	⋯	⋯	−8.49(−70)
$1_0^1 2_0^1 3_0^3$	18 260.28(12)	⋯	⋯	−8.12(13)
$1_0^2 2_0^2$	18 273.73(55)	⋯	⋯	−7.87(−12)
$2_0^1 3_0^5$	18 289.83(59)	⋯	⋯	−8.90(−25)
$1_0^3 3_0^1$	18 298.48(115)	⋯	⋯	−9.66(24)
$1_0^1 2_0^2 3_0^2$	18 298.48(−29)	⋯	⋯	−8.00(−26)
$1_0^2 3_0^3$	18 322.26(23)	⋯	⋯	−10.38(−39)
$2_0^2 3_0^4$	18 326.83(−40)	⋯	⋯	−7.26(43)
$1_0^1 2_0^3 3_0^1$	18 337.40(41)	⋯	⋯	−8.07(38)
$1_0^3 2_0^1$	18 337.40(−25)	⋯	⋯	−8.07(27)
$1_0^1 3_0^5$	18 349.89(30)	⋯	⋯	−9.76(54)
$1_0^2 2_0^1 3_0^2$	18 361.67(−6)	⋯	⋯	−9.06(19)
$2_0^3 3_0^3$	18 365.27(45)	⋯	⋯	⋯
$1_0^1 2_0^1 3_0^4$	18 388.82(14)	⋯	⋯	−10.04(−19)
$1_0^2 2_0^2 3_0^1$	18 401.30(27)	⋯	⋯	⋯
$2_0^1 3_0^6$	18 418.88(40)	⋯	⋯	⋯
$1_0^3 3_0^2$	18 423.98(−11)	⋯	⋯	⋯
$1_0^1 2_0^2 3_0^3$	18 427.67(31)	⋯	⋯	⋯
$1_0^2 3_0^4$	18 449.49(−2)	⋯	⋯	⋯
$2_0^2 3_0^5$	18 456.58(4)	⋯	⋯	⋯
$1_0^3 2_0^1 3_0^1$	18 465.08(60)	⋯	⋯	⋯
$1_0^1 2_0^3 3_0^2$	18 465.08(−56)	⋯	⋯	⋯
$1_0^2 2_0^1 3_0^3$	18 489.46(18)	⋯	⋯	⋯
$1_0^1 2_0^1 3_0^5$	18 517.24(29)	⋯	⋯	⋯
$1_0^2 2_0^2 3_0^2$	18 528.29(−36)	⋯	⋯	⋯

TABLE V. (*Continued.*)

Band	Frequency (cm^{-1})[b]	Isotope shift (cm^{-1})[c] $^{63}Cu^{109}Ag^{197}Au$[d]	$^{63}Cu^{107}Ag^{197}Au$[d]	$^{65}Cu^{109}Ag^{197}Au$
$1_0^3 3_0^3$	18 550.68(8)	...	...	...
$1_0^1 2_0^2 3_0^4$	18 556.07(38)	...	...	...
$1_0^2 2_0^3 1_0^1$	18 568.00(38)	...	...	...
$1_0^2 3_0^5$	18 576.49(− 26)	...	...	...
$2_0^2 3_0^6$	18 585.64(3)	...	...	...
$1_0^3 2_0^1 3_0^2$	18 591.19(12)	...	...	...
$1_0^1 2_0^3 3_0^3$	18 594.12(8)	...	...	...
$1_0^2 2_0^1 3_0^4$	18 617.31(72)	...	...	...
$1_0^3 2_0^2 3_0^1$	18 631.02(− 10)	...	...	...
$1_0^2 2_0^2 3_0^3$	18 656.16(14)	...	...	...
$1_0^1 2_0^2 3_0^5$	18 683.92(12)	...	...	...
$1_0^2 2_0^3 3_0^2$	18 694.69(− 38)	...	...	...
$1_0^3 2_0^1 3_0^3$	18 717.22(− 19)	...	...	...
$1_0^2 2_0^1 3_0^5$	18 743.34(− 32)	...	...	...
$1_0^3 2_0^2 3_0^2$	18 757.06(− 48)	...	...	...
$1_0^2 2_0^2 3_0^4$	18 782.48(− 69)	...	...	...
$1_1^0 3_0^1$	17 378.43(− 18)	0.26(− 39)	0.26(− 9)	− 1.07(− 178)
$2_1^0 3_0^1$	17 448.56(39)	− 0.62(− 36)	0.55(5)	− 0.63(− 108)
2_1^1	17 486.05(− 16)	− 0.04(− 23)	− 0.04(− 53)	0.55(− 16)
3_1^1	17 498.21(67)	− 0.48(− 46)	0.69(52)	− 0.19(23)
$1_1^0 3_0^2$	17 509.93(96)	− 1.25(− 37)	− 1.25(58)	0.23(184)
$1_0^1 2_1^0$	17 552.32(60)	0.13(84)	0.13(39)	...
$2_1^0 3_0^2$	17 578.66(14)	− 0.13(26)	− 0.13(15)	...
$2_1^1 3_0^1$	17 617.27(63)	− 0.68(38)	− 0.68(39)	− 0.69(50)
3_1^2	17 628.64(74)	− 0.36(12)	− 1.56(− 62)	− 1.26(41)
$1_1^0 2_0^1 3_0^2$	17 677.17(− 10)	0.50(76)	− 2.39(− 49)	...
$1_0^1 2_1^0 3_0^1$	17 680.03(− 109)	0.41(− 29)	0.41(42)	0.08(− 14)
$2_1^1 3_0^2$	17 746.69(− 14)	− 0.92(− 35)	− 0.92(23)	− 2.74(− 117)
3_1^3	17 758.39(37)	0.03(34)	− 1.59(10)	− 3.15(− 63)
$1_1^1 2_0^1 3_0^1$	17 778.91(− 69)	...	...	− 2.04(− 6)
$1_0^2 2_1^0$	17 784.53(− 36)	− 0.94(− 25)	− 2.56(− 109)	1.11(203)
3_1^4	17 886.83(− 108)	...	...	...
3_1^5	18 016.85(− 70)	...	...	...

[a] Vibronic bands were fit to the formula,

$$\nu = T_0 + \sum_i [\omega_i' v_i' + x_{ii}(v_i'^2 + v_i')] + \sum_{i<j} x_{ij}'[v_i' v_j' + (v_i' + v_j')/2] - \sum_i \nu_i'' v_i''$$

for $v_i'' = 0,1$. The resulting values of T_0, ω_1', ω_2', ω_3', x_{11}', x_{22}', x_{33}', x_{12}', x_{13}', x_{23}', and ν_1'', ν_2'', and ν_3'' are given in Table VI, along with their 1σ error limits.

[b] Following each observed frequency, the residual $\nu_{obs} - \nu_{calc}$ is given in units of 0.01 cm^{-1} in parentheses.

[c] Isotope shifts are given as ν(isotope modification) − $\nu(^{63}Cu^{107}Ag^{197}Au)$. Following each observed isotope shift, the residual $\nu_{obs} - \nu_{calc}$ is given for the fit of that isotopic modification to the formula given in footnote a. The resulting values of the vibrational constants are given in Table VI, along with their 1σ error limits.

[d] Assignments for the $^{63}Cu^{109}Ag^{197}Au$ and $^{65}Cu^{107}Ag^{197}Au$ species are complicated by the fact that both species fall at mass 369, contributing 67.5% and 32.5% to the intensity of this mass peak, respectively. Accordingly, some of the reported assignments may be in error, particularly for the less abundant species $^{65}Cu^{107}Ag^{197}Au$.

[e] Time-delayed resonant two-photon ionization measurements of the lifetimes of the 014 and 001 levels of $^{63}Cu^{107}Ag^{197}Au$ give $\tau = 585 \pm 170$ and 693 ± 91 ns, respectively (1σ error limits).

all three vibrational excitations in the excited $\tilde{A}$ state are considered. In this way, the strong feature near 17 770 cm^{-1} may be assigned uniquely as the $2_0^1 3_0^1$ band, for example. Likewise, features near 17 834, 17 873, and 17 899 cm^{-1} may be assigned uniquely to the $1_0^1 3_0^1$, $1_0^1 2_0^1$, and $2_0^1 3_0^2$ bands, respectively. By continuing with this sort of analysis and using vibrational constants determined by a fit of the assigned bands to predict positions for the as yet unassigned bands, it is possible to obtain a fairly complete vibrational analysis of the band system shown in Fig. 3. This is presented in Table V, where 75 bands originating from the zero-point level of the ground $\tilde{X}$ state are assigned and fitted to extract the constants T_0, ω_i, and x_{ij} for $^{63}Cu^{107}Ag^{197}Au$.

Finally, a few weak features still remain unexplained. These include two bands to the red of the 0_0^0 band, five very weak, but reproducible features between the 0_0^0 and 3_0^1 bands, and two fairly obvious features between the 3_0^1 and 2_0^1 bands. These are hot bands, arising from molecules which

TABLE VI. Fitted vibrational constants for CuAgAu.[a]

State	Constant	$^{63}Cu^{107}Ag^{197}Au$	$^{63}Cu^{109}Ag^{197}Au$[b]	$^{65}Cu^{107}Ag^{197}Au$[b]	$^{65}Cu^{109}Ag^{197}Au$
$\tilde{A}$	T_0	17 470.84(27)	17 470.54(33)	17 471.41(40)	17 470.10(51)
	ω_1'	235.97(31)	235.22(77)	235.32(94)	235.40(85)
	ω_2'	169.45(31)	168.91(73)	167.27(96)	168.00(76)
	ω_3'	131.52(18)	130.61(42)	130.80(50)	130.56(48)
	x_{11}'	−0.495(63)	−0.57(16)	−0.83(20)	−0.78(17)
	x_{22}'	−0.249(63)	−0.31(15)	0.01(20)	−0.25(15)
	x_{33}'	−0.119(21)	−0.03(5)	−0.16(6)	−0.14(5)
	x_{12}'	−0.444(64)	−0.52(23)	−0.34(32)	−0.51(21)
	x_{13}'	−1.201(40)	−0.93(15)	−1.69(18)	−1.57(14)
	x_{23}'	−0.170(38)	−0.07(15)	0.02(19)	−0.13(12)
$\tilde{X}\,^2A'$	ν_1''	222.83(29)	221.50(33)	222.28(39)	220.41(53)
	ν_2''	153.27(22)	152.29(22)	152.00(26)	150.54(39)
	ν_3''	103.90(28)	102.39(34)	102.68(41)	101.75(57)
χ^2		0.270	0.236	0.331	0.681

[a] All constants are reported in wave numbers (cm^{-1}), followed by the 1σ error limits in parentheses, given according to the number of digits quoted for the parameter. These constants were obtained by a least-squares fit of the data of Table V to the expression

$$\nu = T_0 + \sum_i [\omega_i' v_i' + x_{ii}'(v_i'^2 + v_i')] + \sum_{i<j} x_{ij}'[v_i' v_j' + (v_i' + v_j')/2] - \sum_i \nu_i'' v_i''$$

for $v_i'' = 0,1$.

[b] As mentioned in footnote d of Table V, data for $^{63}Cu^{109}Ag^{197}Au$ and $^{65}Cu^{107}Ag^{197}Au$ were obtained from the same mass peak and there is an associated ambiguity as to what features belong to which species. As a result, the fitted constants should be viewed with caution, particularly for the less abundant $^{65}Cu^{107}Ag^{197}Au$ isotopic modification.

have not been cooled to the vibrational ground state in the supersonic expansion. A careful search of the baseline turns up 17 weak features, which may be ascribed to transitions from three vibrationally excited levels of the ground state. These are also listed in Table V, where five transitions are found to originate from a level about 103.90 cm^{-1} above the ground vibrational level, eight are found to originate from a level 153.27 cm^{-1} above the ground level, and the remaining four transitions originate from molecules with 222.83 cm^{-1} of vibrational energy. A least-squares fit of all of the data listed in Table V then provides the vibrational constants listed in Table VI. The three vibrational frequencies of the ground $\tilde{X}$ state of $^{63}Cu^{107}Ag^{197}Au$ are found to be 222.83 ± 0.29, 153.27 ± 0.22, and 103.90 ± 0.28 cm^{-1}, respectively. These compare with the corresponding values for the excited $\tilde{A}$ state of $\omega_1 = 235.97 \pm 0.31$, $\omega_2 = 169.45 \pm 0.31$, and $\omega_3 = 131.52 \pm 0.18$ cm^{-1}, respectively.

IV. DISCUSSION

A. The $\tilde{A} \leftarrow \tilde{X}$ system of Cu_2Ag

The observed $\tilde{A} \leftarrow \tilde{X}$ band system of Cu_2Ag lies quite far to the red, with its 0_0^0 origin band at 13 188 cm^{-1}. Moreover, the band system possesses a very small intensity, with a fluorescence lifetime of $\tau \approx 30$ μs, corresponding to an absorption oscillator strength of $f \approx 0.0003$. These pieces of information are very helpful in considering the possible assignments of the $\tilde{A}$ excited electronic state. The ground electronic state of Cu_2Ag derives from the interaction of ground state atoms, giving a ground electronic state of either $d^{10}_{Cu,A} d^{10}_{Cu,B} d^{10}_{Ag} 1a_1^2 2a_1^1$, $^2A_1$ or $d^{10}_{Cu,A} d^{10}_{Cu,B} d^{10}_{Ag} 1a_1^2 1b_2^1$, $^2B_2$. In the description of the electronic configurations of these states, the $1a_1$ orbital is taken as a bonding molecular orbital composed of 4*s* orbitals on the copper atoms and a 5*s* orbital on the silver atom without any nodes. The $2a_1$ and $1b_2$ orbitals are similarly composed of $4s_{Cu}$ and $5s_{Ag}$ atomic orbitals, but possess one nodal plane bisecting the Cu–Ag bonds or Cu–Ag–Cu bond angle, respectively. The $d^{10}_{Cu,A} d^{10}_{Cu,B} d^{10}_{Ag} 1a_1^2 2a_1^1$, $^2A_1$ and $d^{10}_{Cu,A} d^{10}_{Cu,B} d^{10}_{Ag} 1a_1^2 1b_2^1$, $^2B_2$ states differ according to whether the third *s* electron of the molecule goes into the $2a_1$ orbital, which has bonding character between the two copper atoms and antibonding character between the copper and silver atoms, or into the $1b_2$ orbital, which is antibonding between the two copper atoms and nonbonding between the copper and silver atoms.

These two states are calculated to be only 0.08 (Ref. 69) or 0.06 eV (Ref. 70) different in energy, with the $^2A_1$ state as the ground state. On the other hand, matrix isolation ESR data on Cu_2Ag isolated in a perdeuterated benzene (C_6D_6) matrix suggest that it possesses a $^2B_2$ ground state, since the data have been analyzed to give a spin population of 41% in the 4*s* orbitals of the two equivalent copper atoms and 5.4% in the 5*s* orbital of the silver atom.[71] This would be consistent with the $d^{10}_{Cu,A} d^{10}_{Cu,B} d^{10}_{Ag} 1a_1^2 1b_2^1$, $^2B_2$ state, in which the unpaired electron occupies a b_2 orbital, which has a node on the silver atom and large amplitude on the two equivalent copper atoms. Of course, perdeuterobenzene may not be an inert matrix material and the energetics of these two states may be perturbed or even reversed by matrix interactions. Regardless of which is truly the ground state, it seems certain on the basis of the calculated energies[69,70] that the $\tilde{A}$ excited electronic state observed in the present study cannot correspond to either of these states.

The remaining candidates for the $\tilde{A}$ state either rearrange the s electron framework by $2a_1 \leftarrow 1a_1$ or $1b_2 \leftarrow 1a_1$ promotions, or promote a d electron to the partially filled s electron orbitals. States which arise from rearrangements of the s electrons can still correlate to the ground state separated atom limit, while the $s \leftarrow d$ promotions must correlate to an excited separated atom limit in which either the copper or the silver atom has been promoted to the d^9s^2, ^2D term. The lowest ^2D terms ($^2D_{5/2}$) in copper and silver lie 11 202.565 and 30 242.26 cm^{-1} above ground state atoms, respectively.[72] For silver, the $5p \leftarrow 5s$ excitation lies at slightly lower energy (29 552.05 cm^{-1}),[72] but neither the $5p \leftarrow 5s$ nor the $4d \leftarrow 5s$ excitation in silver lie low enough in energy to account for the $\tilde{A} \leftarrow \tilde{X}$ transition in Cu_2Ag at 13 188 cm^{-1}. Therefore, we must consider the $\tilde{A}$ state of Cu_2Ag as deriving from either a $4s \leftarrow 3d$ excitation on copper or from a $2a_1 \leftarrow 1a_1$ or $1b_2 \leftarrow 1a_1$ excitation of the s electron framework. The $4s \leftarrow 3d$ excitation in atomic copper (at 11 202.565 cm^{-1}) (Ref. 72) is moved to higher energy (about 20 500 cm^{-1}) (Ref. 73) in Cu_2, since the electron must be excited into an antibonding σ_u^* orbital. For this reason, the $^3\Sigma_u^+ \leftarrow {}^1\Sigma_g^+$ s electron rearrangement ($\sigma_u^* \leftarrow \sigma_g$) requires less energy in Cu_2 than do $\sigma_u^* \leftarrow 3d$ excitations. In triatomic metals such as Cu_2Ag, the $4s \leftarrow 3d$ excitation probably still occurs at a somewhat higher energy than the free atom value of 11 202 cm^{-1} (although not as high as 20 500 cm^{-1}, as found in Cu_2), since the incompletely filled $2a_1$ and $1b_2$ orbitals are still somewhat antibonding in character.

There are problems associated with the assignment of the transition to the $2a_1 \leftarrow 1a_1$ or $1b_2 \leftarrow 1a_1$ excitations of the s electron framework, however. First, both of these excitations are allowed under electric dipole selection rules, and in either case, the transition dipole moment should be quite large, since there is good overlap between the atomic s orbitals. This is not consistent with the long lifetime and small oscillator strength of the observed $\tilde{A} \leftarrow \tilde{X}$ transition. Accordingly, if the transition is assigned as a rearrangement of the s electrons, we must conclude that it is a spin-forbidden transition which gains intensity through spin–orbit contamination of one of the states (presumably the $\tilde{A}$ excited state). Therefore, assuming a rearrangement of the s electrons in the transition, the upper state must be primarily quartet ($S = 3/2$) in character. If this is so, it must have the electronic configuration of $d^{10}_{Cu,A} d^{10}_{Cu,B} d^{10}_{Ag} 1a_1^1 2a_1^1 1b_2^1$, $^4B_2$. However, this state places two of its three s electrons in mildly antibonding orbitals and it would in all likelihood be repulsive. This would not seem to be consistent with the observation of vibrational levels up to 934 cm^{-1} above the zero-point level in Cu_2Ag.

As a result, we believe that the upper state of this system derives from a $4s \leftarrow 3d$ promotion on one of the copper atoms. Nevertheless, the long lifetime of the state probably identifies it as primarily quartet ($S = 3/2$) in character. In the excited state, there will then be four s-type electrons and one d hole. The four s-type electrons could be distributed among the s-based orbitals as $1a_1^2 2a_1^2$, $1a_1^2 1b_2^2$, or $1a_1^2 2a_1^1 1b_2^1$. However, only the last of these can be coupled with the single d hole to give a quartet state. Accordingly, the $\tilde{A}$ state of Cu_2Ag is assigned tentatively as one of the states arising from a $d^9_{Cu,A} d^{10}_{Cu,B} d^{10}_{Ag} 1a_1^2 2a_1^1 1b_2^1$ ($S = 3/2$) configuration. Although this state also has two electrons occupying the mildly antibonding $2a_1$ and $1b_2$ orbitals, just as does the $d^{10}_{Cu,A} d^{10}_{Cu,B} d^{10}_{Ag} 1a_1^1 2a_1^1 1b_2^1$, $^4B_2$ state dismissed above, it nevertheless should be bound because two electrons occupy the bonding $1a_1$ orbital as well.

Although we would like to contribute to a resolution of the controversy over whether the ground state of Cu_2Ag is of $^2A_1$ or $^2B_2$ symmetry, our experimental results are rather insensitive to this point. Collection of a rotationally resolved spectrum, followed by its analysis, would provide a definitive answer to this question, but this is beyond our present experimental capabilities. Essentially the only piece of information that we have established about the $\tilde{X}$ ground state is that it possesses a b_2 vibrational mode with a frequency of 201 cm^{-1}. Unfortunately, the antisymmetric bending frequency has not been calculated by *ab initio* theory, so there is no basis in the present investigation for assigning either the $^2A_1$ or the $^2B_2$ state as the ground state.

B. The $\tilde{A} \leftarrow \tilde{X}$ system of Cu_2Au

The $\tilde{A} \leftarrow \tilde{X}$ band system of Cu_2Au lies further to the blue than that found for Cu_2Ag, where it can be accessed more easily. Nevertheless, it remains difficult to extract much information about the nature of the excited and ground electronic states from the compact spectrum which has been observed. The shorter lifetime observed for this system is consistent with a spin-allowed transition, which would make the upper state a doublet ($S = 1/2$). However, it is not as intense as might be expected for the spin-allowed rearrangements of s electrons, which were discussed for Cu_2Ag above. Accordingly, the $\tilde{A} \leftarrow \tilde{X}$ transition of Cu_2Au is assigned as an $s \leftarrow d$ transition involving the promotion of either a copper $3d$ or a gold $5d$ electron to one of the s-based $2a_1$ or $1b_2$ orbitals. In this case, the d^9s^2, $^2D_{5/2}$ states of both copper and gold are energetically accessible, since they lie 11 202.565 and 9161.3 cm^{-1} above ground state atoms, respectively.[72]

The ground state of Cu_2Au has been calculated to be the $d^{10}_{Cu,A} d^{10}_{Cu,B} d^{10}_{Au} 1a_1^2 2a_1^1$, $^2A_1$ state deriving from ground state atoms, with the $d^{10}_{Cu,A} d^{10}_{Cu,B} d^{10}_{Au} 1a_1^2 1b_2^1$, $^2B_2$ state lying some 4000 cm^{-1} higher in energy.[69] Moreover, the $^2A_1$ state is calculated to have an a_1 bending mode frequency of 163 cm^{-1}, which compares to a calculated value for the $^2B_2$ state of only 116 cm^{-1}.[69] Our measured hot band frequency of 159.73 cm^{-1} is in very close agreement to the value calculated for the $^2A_1$ state, lending support to this assignment of the ground state.

C. The $\tilde{A} \leftarrow \tilde{X}$ system of CuAgAu

The triply mixed triatomic CuAgAu provides a unique case, in that all three vibrational modes are of a' symmetry in the C_s point group and all three have been observed in both the ground and excited states. What is perhaps most surprising is that all three modes *increase* in frequency upon electronic excitation from 103.90 to 131.52, 153.27 to 169.45, and 222.83 to 235.97 cm^{-1}. This is unusual considering that

an additional electron is being placed in one of the antibonding, *s*-based orbitals upon electronic excitation. Such effects have been observed in the $\sigma^* \leftarrow d$ excitations of CuAu (Ref. 61) and Au_2,[63] however, where it was argued that the *d* orbitals of these systems are split into bonding and antibonding pairs. Accordingly, excitation of a strongly antibonding *d* electron into a weakly antibonding σ^* orbital could lead to an increase in vibrational frequency. Presumably similar effects could take place in the CuAgAu molecule, making the excited state somewhat more strongly bound than the ground state, at least as judged by its vibrational frequencies. With this in mind, the $\tilde{A}$ state of CuAgAu is assigned as arising from the promotion of either a copper or a gold *d* electron to one of the unoccupied or partially occupied *s*-based orbitals, which are all of a' symmetry.

In the case of CuAgAu, we need not consider whether the ground state is of $^2A_1$ or $^2B_2$ symmetry, since both of these C_{2v} irreducible representations go into $^2A'$ when the symmetry is degraded to C_s. As a result, there can be no doubt—the ground state of CuAgAu is $\tilde{X}\,^2A'$. Lurking behind this very definite conclusion, however, stands another question: how high in energy is the other low-lying state of $^2A'$ symmetry and where do the conical intersections connecting these two $^2A'$ surfaces lie? The extensive pattern of vibrational levels observed in the $\tilde{A} \leftarrow \tilde{X}\,^2A'$ spectrum of Fig. 3 suggests that a stimulated emission pumping experiment on this molecule should be able to access high vibrational levels of the ground state, and it seems likely that vibrational anomalies associated with this conical intersection may be revealed through such a study. In addition, the $\tilde{A} \leftarrow \tilde{X}\,^2A'$ system of CuAgAu falls in a very convenient spectral region and the intensity of the system suggests that rotationally resolved spectra of the molecule might be obtainable. This would be very exciting, since only a few metal trimers have been investigated with rotational resolution and very little is known about the accuracy of *ab initio* theory in predicting the structures of these species.

V. SUMMARY

Resonant two-photon ionization spectroscopy has been applied to the jet-cooled mixed coinage metal trimers Cu_2Ag, Cu_2Au, and CuAgAu. One electronic band system, designated as the $\tilde{A} \leftarrow \tilde{X}$ system, has been observed for each species. With the exception of Cu_2Au, the spectra display a great deal of vibrational structure (47 assigned bands in Cu_2Ag and 92 assigned bands in CuAgAu), which has been analyzed to give information about the $\tilde{X}$ ground and $\tilde{A}$ excited state vibrational constants. In the case of Cu_2Au, it is thought that predissociation in the $\tilde{A}$ excited electronic state limits the number of vibrational bands which are observed. For all three molecules, it is argued that the excitation removes an electron from a filled $3d^{10}$ subshell of copper (or $5d^{10}$ subshell of gold) and places it in a weakly antibonding *s*-type orbital (of a_1 or b_2 symmetry in Cu_2Ag and Cu_2Au; a' symmetry in CuAgAu). In CuAgAu, this excitation *increases* all three vibrational frequencies, suggesting that the *d* orbitals in this molecule are split into bonding and antibonding orbitals and that an antibonding *d* electron has been excited to a weakly antibonding *s*-type orbital in the process.

ACKNOWLEDGMENTS

We thank Professor William H. Breckenridge for the use of the intracavity etalon employed in the calibration of the dye laser and we thank Jeff Bright for his help in preparing the Cu/Ag and Cu/Ag/Au alloys used as targets in these studies. Research support from NSF under grant number CHE-8912673 is gratefully acknowledged. Acknowledgement is also made to the Donors of the Petroleum Research Fund, administered by the American Chemical Society, for partial support of this research.

[1] D. G. Leopold, J. Ho, and W. C. Lineberger, J. Chem. Phys. **86**, 1715 (1987).
[2] K. M. Ervin, J. Ho, and W. C. Lineberger, J. Chem. Phys. **89**, 4514 (1988).
[3] J. Ho, K. M. Ervin, and W. C. Lineberger, J. Chem. Phys. **93**, 6987 (1990).
[4] K. M. McHugh, J. G. Eaton, G. H. Lee, H. W. Sarkas, L. H. Kidder, J. T. Snodgrass, M. R. Manaa, and K. H. Bowen, J. Chem. Phys. **91**, 3792 (1989).
[5] C. L. Pettiette, S. H. Yang, M. J. Craycraft, J. Conceicao, R. T. Laaksonen, O. Cheshnovsky, and R. E. Smalley, J. Chem. Phys. **88**, 5377 (1988).
[6] O. Cheshnovsky, K. J. Taylor, J. Conceicao, and R. E. Smalley, Phys. Rev. Lett. **64**, 1785 (1990).
[7] K. J. Taylor, C. L. Pettiette, M. J. Craycraft, O. Chesnovsky, and R. E. Smalley, Chem. Phys. Lett. **152**, 347 (1988).
[8] T. N. Kitsopoulos, C. J. Chick, A. Weaver, and D. M. Neumark, J. Chem. Phys. **93**, 6108 (1990).
[9] G. Ganteför, M. Gausa, K.-H. Meiwes-Broer, and H. O. Lutz, Faraday Discuss. Chem. Soc. **86**, 1 (1988).
[10] G. Ganteför, M. Gausa, K.-H. Meiwes-Broer, and H. O. Lutz, Z. Phys. D **9**, 253 (1988).
[11] P. J. Brucat, L.-S. Zheng, C. L. Pettiette, S. Yang, and R. E. Smalley, J. Chem. Phys. **84**, 3078 (1986).
[12] D. Lessen and P. J. Brucat, Chem. Phys. Lett. **160**, 609 (1989).
[13] U. Ray, M. F. Jarrold, J. E. Bower, and J. S. Kraus, Chem. Phys. Lett. **159**, 221 (1989).
[14] M. F. Jarrold and K. M. Creegan, Chem. Phys. Lett. **166**, 116 (1990).
[15] R. L. Hettich and B. S. Freiser, J. Am. Chem. Soc. **107**, 6222 (1985).
[16] R. L. Hettich, T. C. Jackson, E. M. Stanko, and B. S. Freiser, J. Am. Chem. Soc. **108**, 5086 (1986).
[17] M. B. Knickelbein and S. Yang, J. Chem. Phys. **93**, 5760 (1990).
[18] S. Yang and M. B. Knickelbein, J. Chem. Phys. **93**, 1533 (1990).
[19] M. B. Knickelbein, S. Yang, and S. J. Riley, J. Chem. Phys. **93**, 94 (1990).
[20] D. M. Cox, R. L. Whetten, M. R. Zakin, D. J. Trevor, K. C. Reichmann, and A. Kaldor, in *Advances in Laser Science-I*, edited by W. C. Stwalley and M. Lapp (American Institute of Physics, New York, 1986), pp. 527–530.
[21] R. E. Leuchtner, A. C. Harms, and A. W. Castleman, J. Chem. Phys. **94**, 1093 (1991).
[22] E. K. Parks, B. J. Winter, T. D. Klots, and S. J. Riley, J. Chem. Phys. **94**, 1882 (1991).
[23] P. Fayet, A. Kaldor, and D. M. Cox, J. Chem. Phys. **92**, 254 (1990).
[24] D. M. Cox, D. J. Trevor, R. L. Whetten, and A. Kaldor, J. Phys. Chem. **92**, 421 (1988).
[25] J. A. Howard, R. Sutcliffe, and B. Mile, J. Chem. Soc. Chem. Commun. **1983**, 1449.
[26] J. A. Howard and R. Sutcliffe, Surf. Sci. **156**, 214 (1985).
[27] J. A. Howard, K. F. Preston, R. Sutcliffe, and B. Mile, J. Phys. Chem. **87**, 536 (1983).
[28] L. B. Knight, Jr., R. W. Woodward, R. J. Van Zee, and W. Weltner, Jr., J. Chem. Phys. **79**, 5820 (1983).
[29] R. J. Van Zee, C. A. Baumann, and W. Weltner, Jr., J. Chem. Phys. **82**, 3912 (1985).
[30] C. Cosse, M. Fouassier, T. Mejean, M. Tranquille, D. P. DiLella, and M. Moskovits, J. Chem. Phys. **73**, 6076 (1980).

[31] D. P. DiLella, W. Limm, R. H. Lipson, M. Moskovits, and K. V. Taylor, J. Chem. Phys. **77**, 5263 (1982).
[32] D. E. Powers, S. G. Hansen, M. E. Geusic, A. C. Puiu, J. B. Hopkins, T. G. Dietz, M. A. Duncan, P. R. R. Langridge-Smith, and R. E. Smalley, J. Phys. Chem. **86**, 2556 (1982).
[33] Scott Taylor, Eileen M. Spain, and Michael D. Morse, J. Chem. Phys. **92**, 2710 (1990).
[34] Zhenwen Fu, George W. Lemire, Yoon Mi Hamrick, Scott Taylor, Jin-Cheng Shui, and Michael D. Morse, J. Chem. Phys. **88**, 3524 (1988).
[35] Zhenwen Fu and Michael D. Morse, J. Chem. Phys. **90**, 3417 (1989).
[36] Scott Taylor, Eileen M. Spain, and Michael D. Morse, J. Chem. Phys. **92**, 2698 (1990).
[37] A. D. Sappey, J. E. Harrington, and J. Weisshaar, J. Chem. Phys. **88**, 5243 (1988); **91**, 3854 (1989).
[38] J. E. Harrington and J. C. Weisshaar, J. Chem. Phys. **93**, 854 (1990).
[39] J.-P. Wolf, G. Delacrétaz, and L. Wöste, Phys. Rev. Lett. **63**, 1946 (1989).
[40] A. Herrman, M. Hoffman, S. Leutwyler, E. Schumacher, and L. Wöste, Chem. Phys. Lett. **62**, 216 (1979).
[41] G. Delacrétaz and L. Wöste, Surf. Sci. **156**, 770 (1985).
[42] G. Delacrétaz, E. R. Grant, R. L. Whetten, L. Wöste, and T. W. Zwanziger, Am. Phys. Soc. **56**, 2598 (1986).
[43] M. Broyer, G. Delacrétaz, P. Labastie, R. L. Whetten, J.-P. Wolf, and L. Wöste, Z. Phys. D **3**, 131 (1986).
[44] M. Broyer, G. Delacrétaz, P. Labastie, J. P. Wolf, and L. Wöste, Phys. Rev. Lett. **57**, 1851 (1986).
[45] M. Broyer, G. Delacrétaz, G.-Q. Ni, J. P. Wolf, and L. Wöste, Chem. Phys. Lett. **145**, 232 (1988).
[46] M. Broyer, G. Delacrétaz, G.-Q. Ni, R. L. Whetten, J.-P. Wolf, and L. Wöste, J. Chem. Phys. **90**, 843 (1989).
[47] M. Broyer, G. Delacrétaz, G.-Q. Ni, R. L. Whetten, J.-P. Wolf, and L. Wöste, J. Chem. Phys. **90**, 4620 (1989).
[48] Ph. Dugourd, J. Chevaleyre, J. P. Perrot, and M. Broyer, J. Chem. Phys. **93**, 2332 (1990).
[49] H. J. Foth and W. Demtröder, in *Laser Spectroscopy VIII*, edited by W. Persson and S. Svanberg, (Springer, Berlin, 1987), p. 248.
[50] M. M. Kappes, Chem. Rev. **88**, 369 (1988).
[51] P. Radi, Ph.D. thesis, University of Bern, 1986.
[52] M. D. Morse, J. B. Hopkins, P. R. R. Langridge-Smith, and R. E. Smalley, J. Chem. Phys. **79**, 5316 (1983).
[53] W. H. Crumley, J. S. Hayden, and J. L. Gole, J. Chem. Phys. **84**, 5250 (1986).
[54] E. A. Rohlfing and J. J. Valentini, Chem. Phys. Lett. **126**, 113 (1986).
[55] M. D. Morse, Chem. Phys. Lett. **133**, 8 (1987).
[56] P. Y. Cheng and M. A. Duncan, Chem. Phys. Lett. **152**, 341 (1988).
[57] Z. Fu, G. W. Lemire, Y. M. Hamrick, S. Taylor, J. Shui, and M. D. Morse, J. Chem. Phys. **88**, 3524 (1989).
[58] J. R. Woodward, S. H. Cobb, and J. L. Gole, J. Phys. Chem. **92**, 1404 (1988).
[59] J. G. McCaffrey, R. R. Bennett, M. D. Morse, and W. H. Breckenridge, J. Chem. Phys. **90**, 92 (1989).
[60] G. A. Bishea, N. Marak, and M. D. Morse, J. Chem. Phys. **95**, 5618 (1991).
[61] G. A. Bishea, J. C. Pinegar, and M. D. Morse, J. Chem. Phys. **95**, 5630 (1991).
[62] G. A. Bishea and M. D. Morse, Chem. Phys. Lett. **171**, 430 (1990).
[63] G. A. Bishea and M. D. Morse, J. Chem. Phys. **95**, 5646 (1991).
[64] S. C. O'Brien, Y. Liu, Q. Zhang, J. R. Heath, F. K. Tittel, R. F. Curl, and R. E. Smalley, J. Chem. Phys. **84**, 4074 (1986).
[65] S. Gerstenkorn and P. Luc, *Atlas du Spectre d'Absorption de la Molecule d'Iode* (CNRS, Paris, 1978); S. Gerstenkorn and P. Luc, Rev. Phys. Appl. **14**, 791 (1979).
[66] Philip R. Bevington, *Data Reduction and Error Analysis for the Physical Sciences* (McGraw-Hill, New York, 1969), CURFIT program, pp. 235–245.
[67] E. Fermi, Z. Phys. **71**, 250 (1931).
[68] J. Ruamps, C. R. Hebd. Seances Acad. Sci. **239**, 1200 (1954).
[69] S. P. Walch, C. W. Bauschlicher, Jr., and S. R. Langhoff, J. Chem. Phys. **85**, 5900 (1986).
[70] C. W. Bauschlicher, Jr., S. R. Langhoff, and H. Partridge, J. Chem. Phys. **91**, 2412 (1989).
[71] J. A. Howard, R. Sutcliffe, and B. Mile, J. Am. Chem. Soc. **105**, 1394 (1983).
[72] C. E. Moore, Natl. Bur. Stand. Circ. 467 (1952).
[73] M. D. Morse, Chem. Rev. **86**, 1049 (1986).